

## Supporting information for

# Actuation of a Nonconductive Droplet in an Aqueous Fluid by Reversed Electrowetting Effect

Qinggong Wang<sup>\*†</sup>, Meng Xu<sup>†‡</sup>, Chao Wang<sup>†</sup>, Junping Gu<sup>†,§</sup>, Nan Hu<sup>\*\*‡</sup>, Junfu Lyu<sup>§</sup>, Wei Yao<sup>†</sup>

<sup>†</sup> Qian Xuesen Laboratory of Space Technology, China Academy of Space Technology, Beijing 100094, China

<sup>‡</sup> Jilin Province S&T Innovation Center for Physical Simulation and Security of Water Resources and Electric Power Engineering, Changchun Institute of Technology, Changchun 130012, China

<sup>§</sup> Key Laboratory for Thermal Science and Powder Engineering of Ministry of Education, Department of Energy and Power Engineering, Tsinghua University, Beijing 100084, China

Corresponding Authors

\* Email: wangqinggong@qxslab.cn. Tel: +11(86)-10-68113419. Fax: +11(86)-10-68747505.

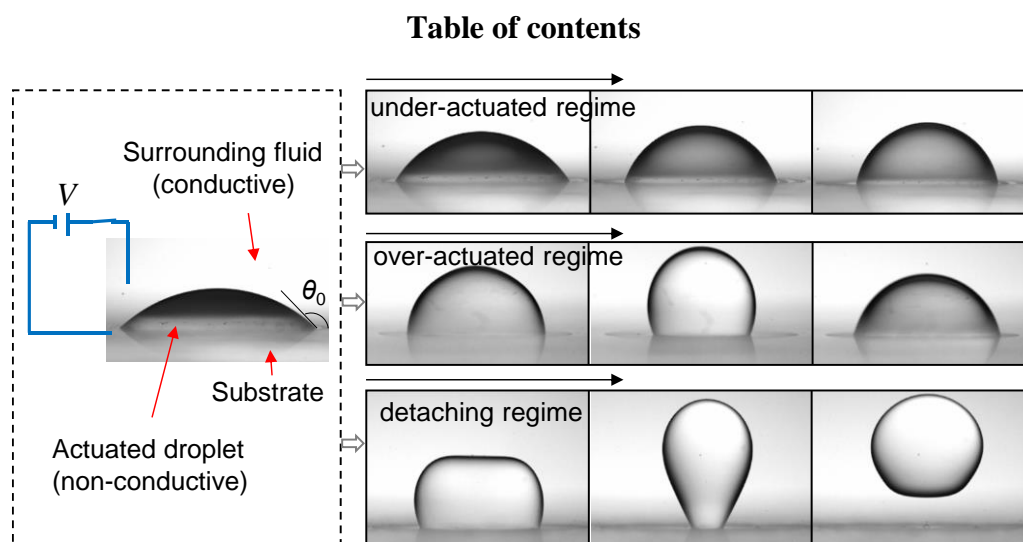
\*\* Email: hn04@tsinghua.org.cn. Tel: +11(86)-431-80578507. Fax: +11(86)-431-80578333.

Number of pages: 4

Number of figures: 5

Number of schemes: 4

Number of tables: 0



## A. Preparation of the solid surface

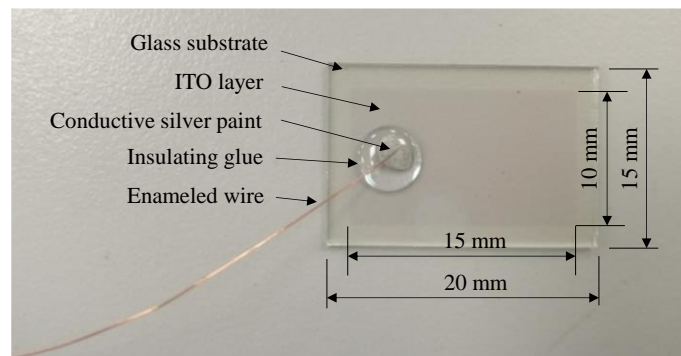


Figure S1. The composite substrate for the REW experiment. The base is a glass plate with dimensions of  $20 \text{ mm} \times 15 \text{ mm} \times 1.1 \text{ mm}$ . A thin indium tin oxide (ITO) film is coated on the upper surface of the glass plate. The ITO film is trimmed at the fringe by a width of 5 mm to avoid electrical breakdown at the sharp edge. Thickness of the coated ITO layer is  $260 \pm 2 \text{ nm}$ , and the surface square resistance is  $\leq 5 \Omega$ . The glass substrate and ITO layer are fabricated commercially with the above designs. Then, we pasted an enameled copper wire on the ITO film by gluing one end of the wire end after trimming the enamel with a conductive silver paint. The silver paint was dried in air for an hour. We pasted a secondary insulating glue on the bounding point to enhance the tightness of the bond. The insulating glue was dried in air for another 24 h. The assembled substrate was cleaned with ethyl alcohol and dried naturally in an ultraclean chamber. Finally, the entire surfaces of the substrate (including the extended copper wire) were deposited by a layer of Parylene C with the chemical vapor deposition (CVD) method. The thickness of the dielectric layer was  $6 \pm 0.5 \mu\text{m}$  as measured by a Step Profiler.

## B. Experimental setups

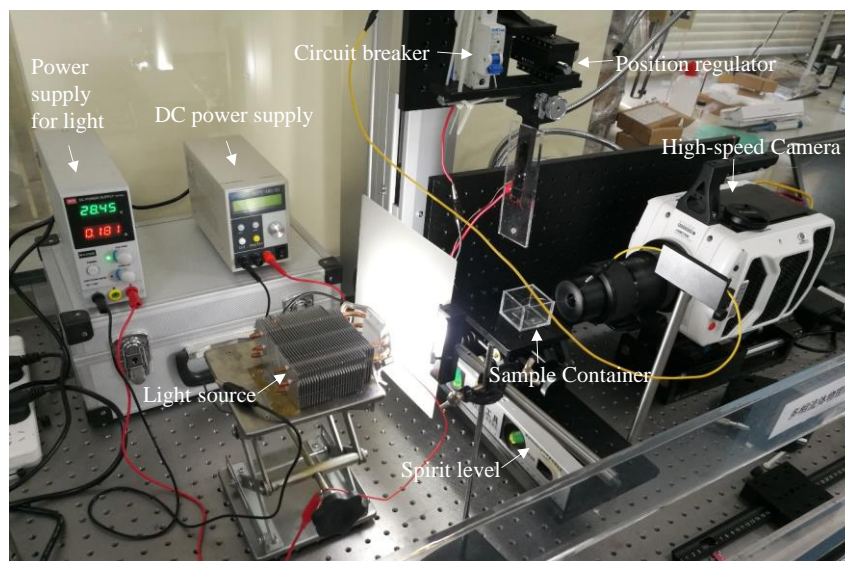


Figure S2. The experimental system is mounted on an optical table and the levelness is checked by a spirit level. The composite substrate is placed into a transparent vessel made of plexiglass which is sit on an operating console. Position of the operating console can be regulated in three-dimensions with the position regulator. The surrounding fluid is filled into the container and the droplet is settled on the solid substrate with a micropipette. The high-speed camera is mounted at one side to capture the deformation of droplets with the help of a light source. The DC power supply provides a potential difference between the solid surface and the surrounding fluid. The applied voltage is tuned from 0 to 400 V by a step of 10 V at a time. Closure of the circuit is controlled by a circuit breaker.

### C. Typical videos and annotations

S1) Video for the underactuated regime with  $\mu_{oil} = 9.35 \text{ mPa}\cdot\text{s}$  and  $V = 110 \text{ V}$ . (a) The actuated period, and (b) the releasing period.

S2) Video for the overactuated regime with  $\mu_{oil} = 9.35 \text{ mPa}\cdot\text{s}$  and  $V = 150 \text{ V}$ .

S3) Video for the detaching regime with  $\mu_{oil} = 9.35 \text{ mPa}\cdot\text{s}$  and  $V = 210 \text{ V}$ .

S4) Video to show the symmetrical actuation of the droplet in the underactuated regime.

**Note:** Both symmetrical and asymmetrical actuations of the droplet are generally seen in the underactuated regime. The video S1 has shown some asymmetrical actuation of the droplet. Asymmetry occurs very likely at low voltages when the pinning force (or adhesive force) is not perfectly and/or symmetrically distributed along the contact line. However, even though the asymmetry occurs, the process is still repeatable. The droplet restores back to its initial position after releasing the voltage, as seen in video S1. In Video S4, we provide extra examples to show the symmetrical actuation of the droplet in the underactuated regime at the same conditions of  $\mu_{oil} = 9.35 \text{ mPa}\cdot\text{s}$  and  $V = 110 \text{ V}$ .

S5) Video to show the effect of the initial contact angle ( $\theta_0$ ) on the onset voltage ( $V_{onset}$ ).

**Note:** In this video, the  $\theta_0$  is manually reduced to  $\sim 30^\circ$  by prewetting the contact area before setting the oil droplet. The droplet spreads further to the prescribed area, leading to a smaller initial contact angle than normal. This video shows that the contact line contracts obviously at a voltage of 40 V. As shown in Figure 3, such a magnitude of contraction can only be achieved at  $V = 50 \text{ V}$  when the  $\theta_0$  is  $\sim 40^\circ$ . So it supports our description in the section *Dynamics of Underactuated Droplets*, ‘Such an effect is proved in our experiment: when we reduced the  $\theta_0$  to  $\sim 30^\circ$ , the  $V_{onset}$  was decreased by about 10 V’

S6) Video to show an example of the droplet collapse at the base in the overactuated regime, with  $\mu_{oil} = 40.94 \text{ mPa}\cdot\text{s}$  and  $V = 150 \text{ V}$ .

S7) Video to show an example of droplet sliding on the solid surface after actuation in the underactuated regime with  $\mu_{oil} = 40.94 \text{ mPa}\cdot\text{s}$  and  $V = 120 \text{ V}$ .

### D. Coefficients of the contact line friction

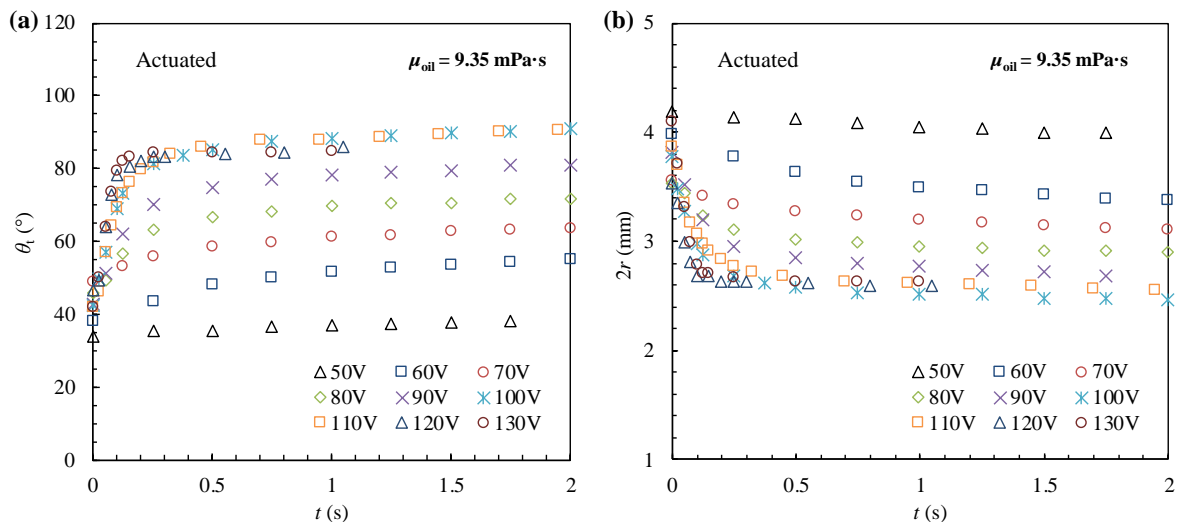


Figure S3. Raw data for typical plots of variation of (a) the transient contact angle ( $\theta_t$ ) and (b) the base diameter of droplet ( $2r$ ) with time ( $t$ ) under different applied voltages, with the droplet volume  $\Delta = 5 \mu\text{L}$  and oil viscosity  $\mu_{oil} = 9.35 \text{ mPa}\cdot\text{s}$ .

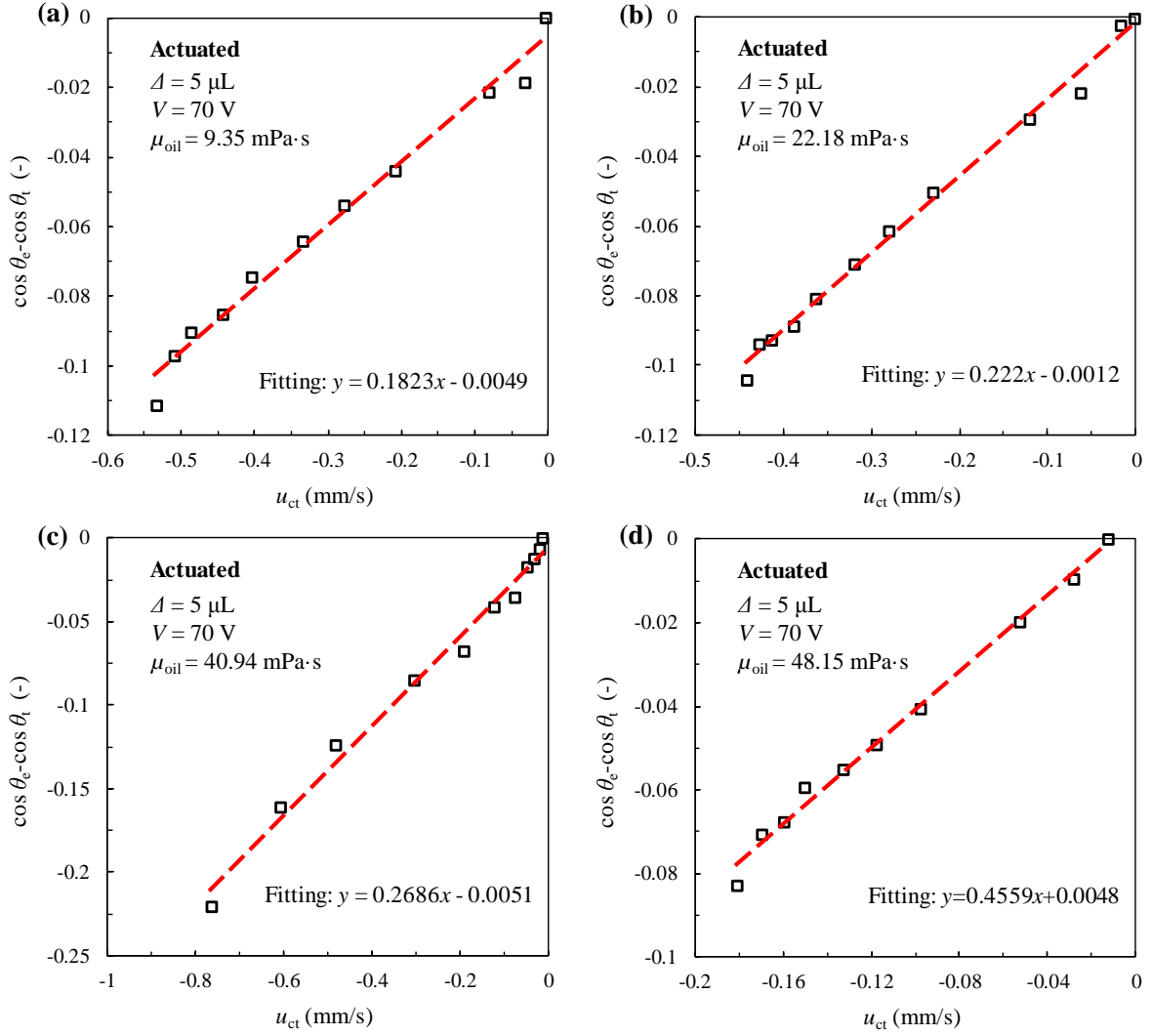


Figure S4. Raw data for representative plots of the  $(\cos \theta_e - \cos \theta_t)$  versus the velocity of the contact line ( $u_{ct}$ ) with (a)  $\mu_{oil} = 9.35 \text{ mPa}\cdot\text{s}$  and  $V = 70 \text{ V}$ , (b)  $\mu_{oil} = 22.18 \text{ mPa}\cdot\text{s}$  and  $V = 70 \text{ V}$ , (c)  $\mu_{oil} = 40.94 \text{ mPa}\cdot\text{s}$  and  $V = 70 \text{ V}$  and (d)  $\mu_{oil} = 48.15 \text{ mPa}\cdot\text{s}$  and  $V = 70 \text{ V}$ . The friction coefficient of the contact line ( $\lambda$ ) can be obtained from the fitting line through  $(\cos \theta_e - \cos \theta_t) = (\lambda/\sigma) \cdot u_{ct}$ .